

# Noise reduction in optical *in situ* measurements for molecular beam epitaxy by substrate wobble normalization

K. A. Bertness,<sup>a)</sup> R. K. Hickernell, S. P. Hays, and D. H. Christensen  
National Institute of Standards and Technology, Boulder, Colorado

(Received 22 December 1997; accepted 27 January 1998)

We demonstrate a normalization method for removing noise introduced into optical *in situ* measurements by sample rotation wobble during molecular beam epitaxy. The technique consists of measuring the angle of rotation of the sample through optical triggers attached to the sample manipulator rotation drive, acquiring a normalization curve at the various trigger points, then applying the normalization appropriate to each trigger to subsequent data. This cyclic normalization is demonstrated on normal-incidence optical reflection data and atomic absorption measurements in which the flux-monitor light beam is reflected from the sample to allow determination of layer thickness in addition to atomic flux. Noise reductions by factors of 3 to 30 were observed in both systems, with the larger improvements for samples with larger wobble angles, while preserving the original time resolution of the data. We achieve normalized optical reflectance data with a noise standard deviation of 1% over a period of one to two hours and similar results for atomic absorption data on shorter time scales. The technique is limited by the long-term mechanical stability of the manipulator and collection optics. [S0734-211X(98)09203-8]

## I. INTRODUCTION

Substrate rotation is used in virtually all molecular beam epitaxy (MBE) growth systems to compensate for spatial variations in source-cell flux. In a typical MBE system, this rotation axis is not aligned perfectly with the sample normal, producing a wobble as the sample rotates. This wobble has no consequences for the materials properties of the layers grown, but it is a significant problem in the application of optical *in situ* monitoring such as atomic absorption (AA) flux measurements and normal-incidence optical reflectance (OR) measurements. The sample wobble causes a light beam reflected off the sample to move as the sample rotates, often resulting in variable light-collection efficiency due to variable shadowing by viewports, cryopanel shrouds, and monochromator slits. Spatial nonuniformities in viewport transmittance and detector responsivity also become important. We have observed noise with amplitudes as large as 50% of the average normal-incidence OR signal for beam wobble angles on the order of  $\pm 0.5^\circ$ . Despite the magnitude of these effects, wobble is not mentioned in any of the literature references we find for application of OR in MBE.<sup>1-3</sup> Most users of *in situ* reflectance techniques either stop sample rotation while taking data, average their data over the period of a rotation cycle, or modify or replace their hardware to reduce wobble.<sup>4</sup> A more sophisticated approach has been demonstrated in which spectral ellipsometry wavelength scans were triggered by the start of a new rotation,<sup>5</sup> though no actual normalization was applied. Wobble noise may account in part for the popularity of optical pyrometry as an *in situ* growth monitoring technique in MBE,<sup>6-9</sup> because pyrometers collect light being emitted from the sample and therefore can be made much less sensitive to wobble.

In conventional AA flux measurements, the light beam

passes above the sample and therefore is not affected by rotation wobble.<sup>10,11</sup> We have shown, however, that combining AA and uv reflectance monitoring in one measurement system by reflecting the uv light beam from the sample enables simultaneous flux and growth rate monitoring of III-V epitaxial growth.<sup>12</sup> The AA data we present here thus have two components—the abrupt changes in transmission from shuttering the atomic flux, which allows us to calculate the growth rate, and interference fringes from multiple reflections at dissimilar material interfaces, which allows us to calculate layer thickness. The flux measurements associated with shutter openings and closings have the particular advantage of being an instantaneous measurement independent of any curve fitting or refractive index calculations. Although reflection-mode AA has the advantage of measuring layer thickness as well as atomic flux, it is also sensitive to sample wobble.

In this article, we focus on a method of removing the wobble-induced noise that begins with the collection of a normalization curve at several trigger points, each of which corresponds to a particular angular position of the substrate as it rotates. The normalization curve is acquired while the substrate reflectance is constant, such as during a growth interruption or at the end of a thick layer. Subsequent data are normalized by dividing each point by the normalization curve point that corresponds to the same trigger index and hence to the same rotation phase angle. We call this technique “cyclic normalization” to distinguish it from other possible schemes that we mention above; its primary advantages are its simplicity and its retention of the original time resolution of the data. Cyclic normalization reduces the noise in OR by a factor of 7 or more. In AA measurements, the noise is reduced by 3 to 30 times, with the larger reductions occurring for samples with larger wobble. Key factors in making this technique work successfully have been careful

<sup>a)</sup>Corresponding author; electronic mail: bertness@boulder.nist.gov

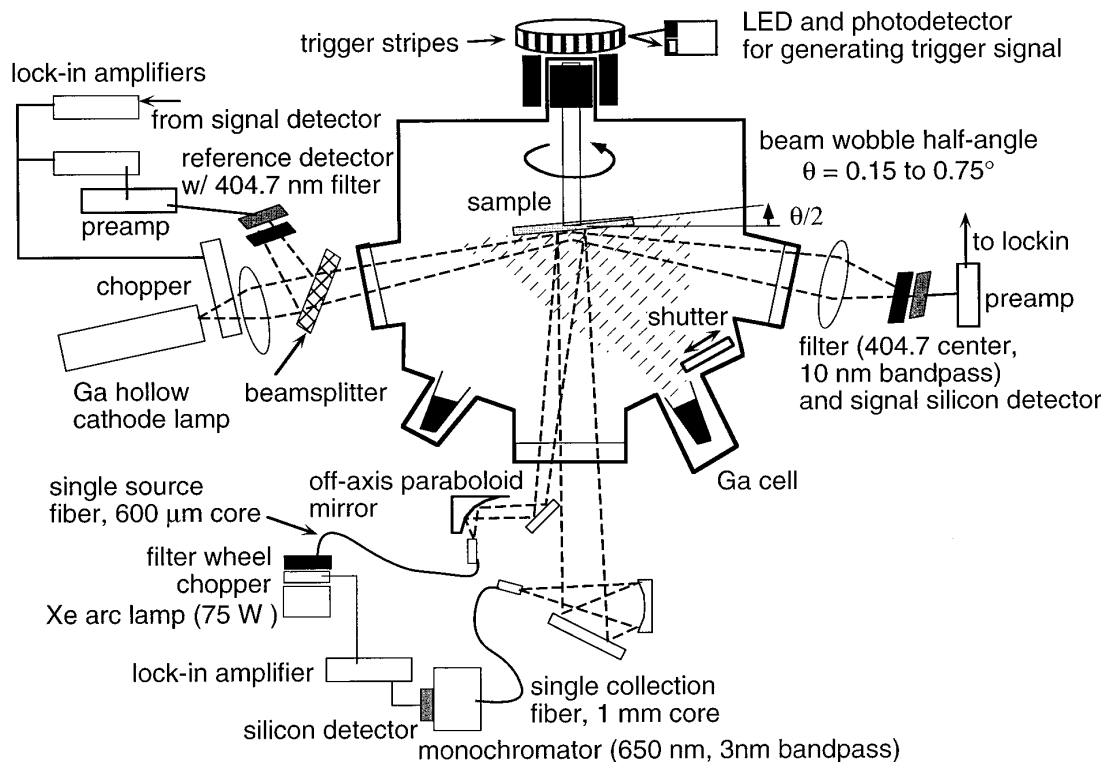


FIG. 1. Experimental setup and operating parameters for *in situ* AA and OR systems. The sample wobble is shown greatly exaggerated for illustration purposes.

budgeting of data acquisition and computer processing time in order to perform the normalization in real time, the use of several triggers per rotation to allow accurate normalization despite rotation speed variations, and conscious design of optical collection systems to minimize the effects of mechanical vibration. Efforts to modify substrate holders to achieve smaller wobble angles or to modify optics to achieve higher light collection efficiency are also well rewarded. Our systems are currently limited in terms of the long-term stability of the normalization, and we discuss some possible improvements at the end of this article.

## II. EXPERIMENTAL SETUP

A schematic description of the OR spectroscopy and AA measurement equipment is given in Fig. 1. The sample is 36 cm from each of the AA ports and 65 cm from the normal-incidence port. The AA beam is incident at an angle of about  $78^\circ$  with respect to the substrate normal, while the OR beam is offset just slightly ( $\approx 0.5^\circ$ ) from the normal to help separate the outgoing and incoming beams. The AA beam projects a spot about 20 mm wide and 90 mm long where it intersects the sample surface. The OR beam increases in diameter from roughly 10 to 20 to 30 mm at the entrance point on the window, at the sample, and at the exit point on the window, respectively. This residual divergence of about  $1^\circ$  is due to imperfections in the off-axis parabolic mirror. At large wobble angles, both systems experience reduction in collection efficiency of the reflected beam from shadows of the cryopanel openings inside the vacuum chamber and

movement of the collected beam partially off the detector. The vacuum chamber windows are heated to 250 to  $300^\circ\text{C}$  to prevent deposits of As that otherwise would decrease transmittance over time.

The Ga hollow cathode lamp emits light at multiple spectral lines, so bandpass filters are used to limit the sensitivity of the detectors to a Ga atomic emission line at 403.3 nm. To account for variation in the lamp's intensity, a beamsplitter in the AA system reflects a portion of the uv beam into a reference detector, the signal of which is used to normalize the transmission signal digitally. The OR system lacks this feature, so variations in the arc-lamp intensity contribute to the random noise and drift in the signal. The relative AA signal is calculated by dividing the raw AA signal by the signal value measured at the beginning of each run on a bare GaAs substrate with no Ga flux present. The ratio  $A$  of the relative AA signal with the Ga shutter open to the relative AA signal with the Ga shutter closed is calibrated against the growth rate  $G$  as measured by reflection high-energy electron diffraction (RHEED) over  $G$  values of 0.3 to 1.1 monolayers/s to yield the curve  $G = -21 \ln(A) - 0.073$  in that range. RHEED calibration data is taken just before the AA measurements on a separate,  $1\text{ cm}^2$  sample for greater accuracy. In the absence of changes in the reflectance of the sample, the relative AA signal is proportional to the beam transmittance, and therefore the logarithm of  $A$  is expected to be a linear function of the growth rate.<sup>10</sup> The deviation from linear proportionality near zero growth rate has been observed previously.<sup>11</sup>

The maximum half-angle  $\theta_w$  of the beam wobble is quantified by measuring the approximate radius of the path traced by a laser beam reflected from the sample through the normal-incidence port. By this definition,  $\theta_w$  is equal to twice the half-angle of the wobble of the sample normal about the rotation axis (see Fig. 1). The technique has an uncertainty of  $\pm 0.02^\circ$ . The rotation-angle trigger signal is generated by measuring reflectance from a piece of transparency film having 18 trigger stripes that encircle the substrate manipulator rotation magnet. We generate the trigger signal with an interlock photosensor that is part of the transfer system for our growth machine. Two of the stripes are about 30% closer together than the others to provide a rotation phase reference point for determining a zeroth trigger. The AA and OR signals accomplish the triggering in slightly different ways. To acquire AA data, the analog-to-digital converter on the data acquisition system is triggered by the leading edge of the trigger signal, providing eighteen data points per cycle, each of which is an average of 10 points taken at a high data rate immediately after the rising edge of the trigger. No use is made of the zeroth trigger. A normalization curve is generated at the beginning of each data set by averaging the values of the first five cycles of triggered data.

The OR data acquisition system reads both the trigger and signal voltages at 400 Hz, then processes the trigger voltages with software to keep one data point for each leading and falling trigger edge, yielding 36 data points per cycle. Each of these points is the average of three signal points surrounding the trigger edge. The OR software trigger detection also identifies zeroth triggers and stores a trigger index number for each signal point. Even though feedback control of layer growth can be at a much lower frequency (1 Hz), a moderately high-speed data acquisition rate (100 Hz or more) is essential to both techniques because of the need to accurately follow the normalization curve through unpredictable changes in the substrate rotation speed (approximately 15%). Data acquisition using a general purpose interface bus (GPIB) interface, for example, is not adequate for real-time trigger detection. Although the zeroth trigger feature is convenient for postgrowth data analysis and long-term stability studies, in practice we find that neither system misses triggers.

All experiments are carried out in a commercial single-wafer molecular beam epitaxy machine. The entire growth chamber is tilted relative to the horizontal by about  $25^\circ$  so that the substrate faces downward and the sources face upward. The substrate holders are held by three pins on the manipulator that lock into three slots on the substrate holder outer ring. The three-pin design provides for good stability as the three pins define a single plane for the ring to rest upon. All the data in this article are taken on 50 to 52-mm-diam GaAs substrates that must be attached to the substrate holder ring with spring plates. The plates themselves contain fingers and alignment notches that can alter the tilt of the substrate relative to the outer ring, and we have found considerable variation in the beam wobble angle seen with three different outer rings and spring plate pairs. Sample rotation speed is  $0.16 \pm 0.02$  Hz (10 rpm) unless stated otherwise.

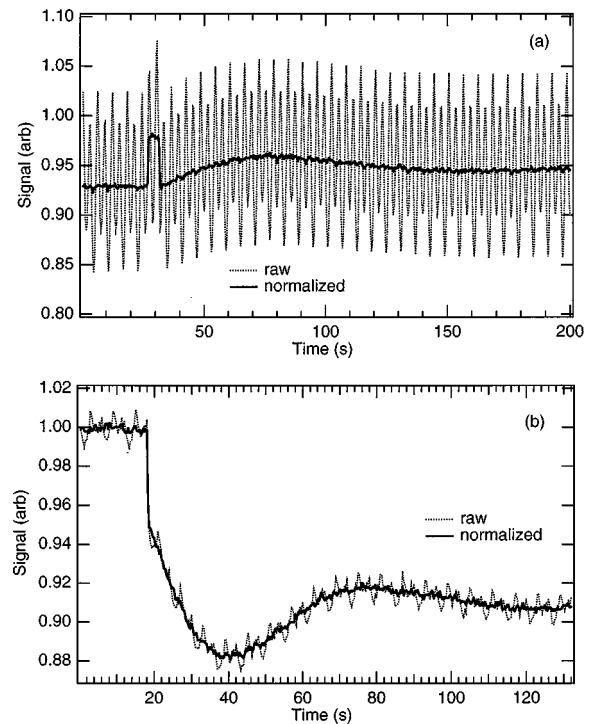


FIG. 2. AA data both with and without cyclic normalization. (a) Data for large beam wobble ( $\theta_w = \pm 0.75^\circ$ ), showing how normalization reveals the growth interruption near 30 s and the optical interference fringe (peak near 80 s) from growing GaAs on AlGaAs. The standard deviation  $\sigma_G$  of the calculated growth rate is reduced from 110% to 3% by the normalization method. (b) Data for AlGaAs on GaAs for a sample with small beam wobble ( $\theta_w = \pm 0.15^\circ$ ), showing  $\sigma_G$  reduction from 10% to 3% by the normalization method. The time interval from 0 to 19 s corresponds to a growth interruption.

### III. EXPERIMENTAL RESULTS

Figures 2 and 3 illustrate the basic utility of the cyclic normalization method in AA and OR, respectively. Figure 2(a) shows raw and normalized AA data, taken during the growth of GaAs on  $\text{Al}_{0.29}\text{Ga}_{0.71}\text{As}$  with a beam wobble  $\theta_w = \pm 0.75^\circ$ . The important features of the data are masked by the 20% peak-to-peak wobble noise in the raw data. In the last section of this curve, where the interference oscillations have damped out, the calculated growth rate had a peak-to-peak uncertainty of 390% and a standard deviation  $\sigma_G$  of 110% relative to a smooth curve drawn through the data. When the cyclic normalization method is applied, the Ga shutter flips from a brief growth interruption near 30 s and the reflectance interference fringe peak at about 80 s become clear. The standard deviation  $\sigma_G$  is reduced by a factor of 30 through cyclic normalization to 3%. During a run for which  $\theta_w = \pm 0.15^\circ$ ,  $\sigma_G$  was reduced from 10% to 3% by applying cyclic normalization, as shown in Fig. 2(b).

Figure 3 shows sections of OR data from the beginning and end of a run for which  $\theta_w = \pm 0.15^\circ$ . The effectiveness of the cyclic normalization is quantified by smoothing the data, calculating the differences of the data points (raw or normalized) from the smooth curve, and then converting the differences to a percentage of the corresponding smooth-curve points. The standard deviation  $\sigma_{\text{OR}}$  of these percentage dif-

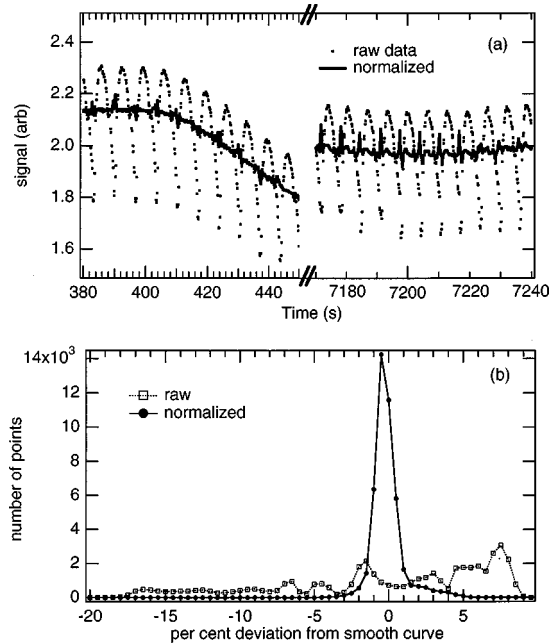


FIG. 3. (a) OR data with and without cyclic normalization taken at the beginning of a run, just after generation of the normalization curve, and about two hours later in the same growth run, for which  $\theta_w = \pm 0.15^\circ$ . The standard deviation  $\sigma_{OR}$  for the entire data set is reduced from 7.1% to 1.0% by the cyclic normalization. (b) A histogram of the percent deviations for the sample in (a), showing how cyclic normalization both reduces the standard deviation and produces a more classic noise distribution.

ferences is reduced by about a factor of 7 from 7.1% to 1.0% by cyclic normalization. Data from different run for which  $\theta_w = \pm 0.6^\circ$  shows standard deviation  $\sigma_{OR}$  reduction from 10% to 1.3%. The change in wobble noise distribution is illustrated in more detail in the histograms in Fig. 3(b) showing the number of points in each curve with specific percent-age differences from a smooth curve.

These graphs show that the cyclic normalization method dramatically reduces the effect of wobble in both kinds of optical *in situ* data without any loss in time resolution. The remaining noise in the normalized curves in Fig. 3(a), however, still has a significant cyclic component that grows in time. The effectiveness of cyclic normalization in the OR system degrades rapidly in the first 100 to 300 s after acquisition, and then stabilizes at  $\sigma_{OR} \approx 1\%$ , although it may continue to grow slightly over several hours. The wobble noise in the AA system in its current configuration typically reaches unacceptable levels within 0.5 to 10 min of normalization curve acquisition. It is not practical to acquire a new normalization curve every 100 s, though periodic updates in conveniently placed growth interruptions would be both possible and valuable in longer runs. The AA system is more difficult to stabilize because the growth rate is derived from only about 5% of the relative AA signal for  $G=1$  monolayer/s. The reflectance noise in the AA signal is thus multiplied by a factor of 20 in calculating the growth rate.

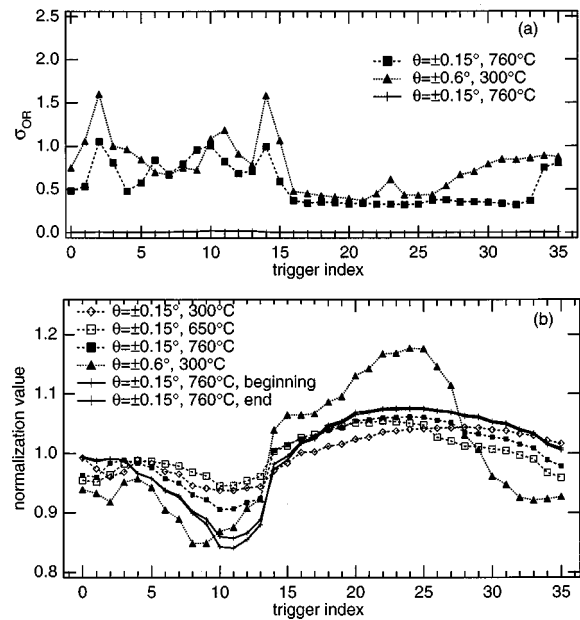


FIG. 4. (a) Standard deviation  $\sigma_{OR}$  for partial data sets grouped by trigger index number, showing that certain regions of the rotation curve are noisier than others. This data along with other evidence suggest that there is some irregular rubbing in the substrate manipulator. (b) Normalization curves used for the runs characterized in (a), with some additional curves showing the effect of substrate manipulator heating and long-term instability. Temperatures given are for the manipulator thermocouple setpoint; GaAs wafer temperature as measured by an optical pyrometer is about 600 °C for the 760 °C thermocouple setpoint.

#### IV. DISCUSSION

A large part of the cyclic noise arises from anomalies in the rotation of our particular substrate manipulator. In the laser beam measurements of  $\theta_w$ , we observe that the reflected beam does not follow a perfectly circular path, but rather has distinct angular discontinuities, indicating that the internal drive magnets are sometimes rubbing against the manipulator tube walls. Vibrations can be felt on the external parts of the manipulator as the sample rotates through these sections of its cycle. As further proof, we note that the irregularities persisted even after installing new set of rotary bearings, and score marks were observed on one of the magnets. These portions of the cycle where irregular rubbing occurs are evident in Fig. 3(a). This effect is presented more systematically for a few different runs in Fig. 4(a), where  $\sigma_{OR}$  is calculated separately for data points corresponding to each different trigger index point. Another indication of manipulator mechanical instabilities is that the normalization curves shift noticeably with substrate temperature, as shown by the open symbols in Fig. 4(b). Finally, we also observe that AA data noise increases with rotation speed ( $\sigma_G = 3\%$ , 4%, and 7% for rotation speeds of 0.08, 0.16, and 0.24 Hz), again pointing to irregular vibrations in the manipulator.

In addition to mechanical effects in the substrate manipulator, mechanical vibrations of the optical components may also contribute to the change in the shape of the normalization curves and consequent degradation of the normalization

effectiveness. As a specific example, the OR has considerably less long-term stability when the reflected light is gathered by a 7 fiber, circular-to-rectangular bundle rather than a single large-core fiber. In the bundle configuration, the substrate wobble causes the focused reflected beam to trace a circle over the different fibers with partial blockage in the dead regions between fibers. Small changes in the positioning and focus of the reflected beam onto the bundle therefore lead to changes in the normalization curve shape. Further improvements in mechanical stability and optical collection efficiency are thus likely to improve the long-term stability of both systems, particularly the AA system. We anticipate that the ultimate growth-rate-equivalent noise limit for our AA system to be at least as low as 0.3%, a value measured during an *ex situ* test of the AA system on a vibration isolation table. Using AA methods that do not reflect light off the sample surface, other researchers have reduced the short-term (5 s time scale) uncertainty in growth rate to 0.25% by real-time feedback to the lamp power control.<sup>10</sup> Laser-based AA measurement systems offer some advantages as well, including advanced spectroscopic techniques for increased sensitivity and drift correction.<sup>13</sup>

The cyclic normalization procedure outlined here has been shown to give significant reduction of noise introduced by the sample wobble. There are some possible improvements suggested by our results. The optics collection efficiency and mechanical stability can be improved in both systems. A laser light source for AA measurements would make 100% collection efficiency attainable while increasing the average power. The manipulator magnet clearance must be increased to avoid the irregularities caused by the rubbing of the magnet against the housing. We also believe that it should be possible to decrease the beam wobble from all of our 52 mm substrate holders to  $\theta_w = \pm 0.2^\circ$  or less by adjusting the fingers in the front spring plate. Finally, the trigger strip could be replaced by an optically encoded rotation drive motor with an analog position readout for more detailed mapping of the normalization curve.

The answer to the more general question of how useful the cyclic normalization method is dependent on the ultimate application to epitaxial crystal growth control. Even without any further improvements, cyclic normalization is an adequate technique for preparing raw data for fitting to interference fringe curves and determining growth rate. Even though the demands on AA mechanical stability are greater than for OR, the AA system is also easier to rezero periodically, and some short, occasional checks are sufficient to assure growth rate stability during long growth runs. If the rotation anomalies in our manipulator are in fact responsible for most of our long term stability limitations, then other MBE growth systems with more reproducible wobble should experience even better results using cyclic normalization. The standard deviation  $\sigma_{OR}$  averaged over the entire rotation cycle, for example, drops from about 1.0% to below 0.5% if the noisy trigger region is excluded from consideration. Even with flawed equipment, it may be more desirable to ignore data from part of the rotation cycle than to average over an

entire cycle because the former approach retains better time resolution.

If the cyclic normalization drift in our OR and AA systems induced by mechanical instabilities is not in fact improved by our proposed modifications, then we can consider more sophisticated digital signal processing techniques, such as filtering out the higher frequency components corresponding to the rotation frequency and its higher harmonics with Fourier transforms. The data we have now are not well suited for Fourier analysis because of the low effective sampling rate, and yet data files covering 2 h of growth are 2 Mbytes in length. An effective Fourier analysis approach must therefore include real-time analysis on temporarily stored data. Proper windowing of the data to retain the low frequency components will be difficult, and any frequency components near the rotation frequency harmonics will out of necessity be lost.

## V. CONCLUSIONS

Cyclic normalization of optical *in situ* monitoring data from both atomic absorption and normal-incidence optical reflectance systems significantly reduces the wobble-induced rotation noise with no loss in time resolution. We have achieved noise standard deviations of 1% or less in normalized optical reflectance data over a period of one to two hours and similar results for atomic absorption data on shorter time scales. The resulting normalized data are adequate for growth rate determination from both techniques. Reducing mechanical instabilities, many of which may be peculiar to our substrate manipulator, will improve the long-term stability of the cyclic normalization technique.

## ACKNOWLEDGMENT

Contribution of National Institute of Standards and Technology.

<sup>1</sup>D. E. Aspnes *et al.*, J. Cryst. Growth **120**, 71 (1992).

<sup>2</sup>V. Bardinal, R. Legos, and C. Fontaine, Appl. Phys. Lett. **67**, 244 (1995).

<sup>3</sup>J. V. Armstrong, T. Farrell, T. B. Joyce, P. Kightley, T. J. Bullough, and P. J. Goodhew, J. Cryst. Growth **120**, 84 (1992).

<sup>4</sup>C. H. Kuo, S. Anand, R. Droopad, K. Y. Choi, and G. N. Maracas, J. Vac. Sci. Technol. B **12**, 1214 (1994).

<sup>5</sup>F. G. Celii, Y.-C. Kao, A. H. Katz, and T. S. Moise, J. Vac. Sci. Technol. A **13**, 733 (1995).

<sup>6</sup>A. J. SpringThorpe, T. P. Humphreys, A. Majeed, and W. T. Moore, Appl. Phys. Lett. **55**, 2138 (1989).

<sup>7</sup>Y. M. Houn, M. R. T. Tan, B. W. Liang, S. Y. Wang, and D. E. Mars, J. Vac. Sci. Technol. B **12**, 1221 (1994).

<sup>8</sup>H. P. Lee, Y. Li, D. L. Sato, and J. J. Zhou, J. Vac. Sci. Technol. B **14**, 2151 (1996).

<sup>9</sup>R. N. Sacks, R. M. Sieg, and S. A. Ringel, J. Vac. Sci. Technol. B **14**, 2157 (1996).

<sup>10</sup>S. A. Chalmers and K. P. Killeen, Appl. Phys. Lett. **63**, 3131 (1993).

<sup>11</sup>P. Pinsukanjana, A. Jackson, J. Toffe, K. Maranowski, S. Campbell, J. English, S. Chalmers, L. Coldren, and A. Gossard, J. Vac. Sci. Technol. B **14**, 2147 (1996).

<sup>12</sup>K. J. Knopp, J. R. Ketterl, D. H. Christensen, T. P. Pearsall, and J. R. Hill, Mater. Res. Soc. Symp. Proc. **441**, 761 (1996).

<sup>13</sup>W. Wang, M. M. Fejer, R. H. Hammond, M. R. Beasley, C. H. Ahn, M. L. Bortz, and T. Day, Appl. Phys. Lett. **68**, 729 (1996).